Journal of Molecular Catalysis A: Chemical 332 (2010) 7–12

Contents lists available at ScienceDirect

Journal of Molecular Catalysis A: Chemical

journal homepage: www.elsevier.com/locate/molcata

Editor's Choice paper

Catalytic nanoreactors for ester hydrolysis

Alexanders T.N. Berlamino, Elisa S. Orth, Renata S. Mello, Michelle Medeiros, Faruk Nome*

Departamento de Química, INCT-Catálise, Universidade Federal de Santa Catarina, Florianópolis, SC 88040-900, Brazil

ARTICLE INFO

Article history:
Received 7 June 2010
Received in revised form 25 August 2010
Accepted 2 September 2010
Available online 21 September 2010

Keywords:
Ester hydrolysis
Ionenes
Nanoreactors

ABSTRACT

Hydrolysis of 4-nitrophenyl benzoate (PNPB) in the presence of ionene nanoreactors was studied comparing the ionenes, poly[(dimethyl)-2-hydroxy propanodiyl chloride] (2-OH-33R1), poly[(methylbutyliminium)-2-hydroxy propanodiyl chloride] (2-OH-33R4) and poly[(methyloctyliminium)-2-hydroxy propanodiyl chloride] (2-OH-33R8). Methyl orange incorporation and study of viscosity showed that increase of the side chain length of the ionene enhances the ability to form globular hydrophobic microdomains. Catalytic hydrolysis of PNPB follows the order 2-OH-33R8 ≫ 2-OH-33R4 > 2-OH-33R1, and 2-OH-33R8 has the lowest pK_a that may reflect its higher hydrophobicity, which apparently influences the ionene nanoreactor reactivity. A lower pK_a indicates easier deprotonation of the alkoxide group, which participates more effectively in the reaction and the 2-OH-33R8 functionalized ionene acts as a specially effective catalytic homogeneous nanoreactor.

1. Introduction

The design of efficient nanoreactors based on the mimicking of enzymatic reactions has been of increasing interest and resulted in the design of efficient models, ranging from a simple molecular structures [1–5] to more complex macromolecules (polymeric [6] and dendrimeric [7]), which combine different functionalities that resemble polysoaps and natural enzymes [8–11]. Polysoaps are a class of polymers which comprise features of polyelectrolytes and micelles, thus forming well-organized structures which depend on electrostatic and hydrophobic forces and allow the binding of organic substrates and ionic reactants [12]. A typical polysoap is obtained when polyvinylpyridine is alkylated with ethyl and dodecyl bromides [13], and this class of compounds can accelerate many reactions [13,14], resembling the well established rate effects of micelles. The alkaline hydrolysis of 4-nitrophenyl hexanoate in the presence of the copolymer formed from 4-vinyl-N-ethylpyridinium bromide and 4-vinyl-N-dodecylpyridinium bromide (8×10^{-4} M, expressed as monomeric units) is accelerated by up to 14-fold, compared to reaction in absence of the polysoap [13]. Micellar catalysis acceleration (dodecyltrimethylammonium bromide) of the same reaction proceeds with a factor of less than 3, at a much higher concentration (0.02 M) [15].

An interesting class of polysoaps are the ionenes, which are cationic polymers with quaternized nitrogen atoms in the polymer backbone separated by different numbers (x, y) of methylene groups. The hydrophobicity of these compounds is determined by the number of the methylene group in the spacers and the size of the side chain segment, forming polysoaps aggregates, which in many aspects are similar to micelles [16–18].

Ionenes have found a variety of applications, such as fungicides and bactericides [19,20], anticoagulants [21], antiheparinic agents [22], flocculants [23] and corrosion inhibitors [24]. Most recently, ionenes have been shown to have relevance as gene delivery agents [8,25,26], because use of cationic polymers in non-viral gene delivery is of increasing interest due to safety considerations [27].

Ionenes may be functionalized with reactive groups, thus behaving like a nanoreactor. We reported previously the hydrolysis of benzoic anhydride mediated by micelles and ionene nanoreactors [28]. In particular, the functionalized poly[(dimethyl)-2-hydroxy propanodiyl chloride] (2-OH-33R1) gave up to 25-fold rate enhancements, in contrast to the 5-fold rate enhancement for the non-functionalized ionene poly[(dipropyliminium)-1,3-propanediyl bromide] (33R3), showing the important participation of the ionene alkoxy group.

In this study, we are interested in evaluating the effect of the introduction of hydrophobic microdomains in 2-OH-33R1, with ionene nanoreactors such as poly[(methylbutyliminium)-2-hydroxy propanodiyl chloride] (2-OH-33R4) and poly[(methyloctyliminium)-2-hydroxy propanodiyl chloride] (2-OH-33R8). The effect of the increase in hydrophobicity is analyzed by examining reduced viscosity, methyl orange incorporation, and kinetic effects. Alkaline hydrolysis of 4-nitrophenyl benzoate is efficiently mediated by the functionalized ionenes

* Corresponding author. Tel.: +55 48 3721 6849; fax: +55 48 3721 6850.
E-mail address: faruk@qmc.ufsc.br (F. Nome).

1381-1169/$ – see front matter © 2010 Elsevier B.V. All rights reserved.
doi:10.1016/j.molcata.2010.09.002

which concentrate reagents and behave as catalytic homogeneous nanoreactors.

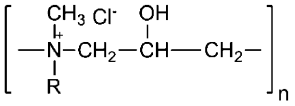

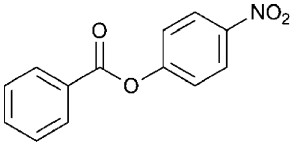

PNPB

2-OH-33R1 R = $-CH_3$

2-OH-33R4 R = $-(CH_2)_2-CH_3$

2-OH-33R8 R = $-(CH_2)_7-CH_3$

2. Experimental

2.1. Materials

Reactants, methylamine 40%, bromobutane 98% and bromodecane were obtained from Merck. Methylbutylamine 99% and diethylamine were from Aldrich and α-epichlorohydrin was from Sigma. All these reactants were used as received. Other reactants and solvents of analytical grade were used without further purification. The ionene 2-OH-33R1 was prepared and purified as described [23,28]. The syntheses of 2-OH-33R4 and 2-OH-33R8 are described in the supplementary information.

2.2. Potentiometric titration

The polymer concentrations in the stock solutions were determined by titration of the chloride counterion by using the Mohr method. Standard solutions were 0.1 M silver nitrate and silver chromate was the indicator. The concentration of polymers, expressed as monomeric units, was 93.5 mM, 56.0 mM and 1.75 mM for 2-OH-33R1, 2-OH-33R4 and 2-OH-33R8, respectively.

2.3. Kinetics

Reactions were followed in aqueous solution, at constant pH, by UV–vis spectrometry measuring the appearance of p-nitrophenolate ion at 400 nm. All reactions were in 0.01 M borate buffer and first order rate constants, k_{obs}, were not affected by this dilute buffer [29]. The reactions were carried out in quartz cuvettes with a final volume of 3.0 mL and 50 μM of PNPB. Temperature was maintained at 25 °C with a thermostatted water-jacketed cell holder. First order rate constants, k_{obs}, were calculated from linear plots of $\ln(A_\infty - A_t)$ against time for at least 90% reaction with an iterative least-squares program and correlation coefficients were >0.999 for all kinetic runs. Ionene solutions were prepared with deionized H_2O (Milli-Q system, Millipore).

2.4. Viscosity

Viscosities of aqueous solutions of the ionenes 2-OH-33R8 and 2-OH-33R4 were carried out in an Ostwald viscometer at 25 °C. The initial ionene solution (1.18×10^{-2} M of 2-OH-33R8 and 3.27×10^{-2} M of 2-OH-33R4) was progressively diluted with water, and the viscosity measured after each dilution. Standard solutions of water, ethanol, acetone and chloroform were used to calibrate the instrument.

2.5. Dye incorporation

The absorption spectra of methyl orange in a borate solution (2×10^{-2} M) were determined at pH 9.4, and showed a maximum at 464 nm. Aliquots of 10 μL of a stock solution 1×10^{-2} M of methyl orange were added to a cuvette containing 2.0 mL of the desired polyelectrolyte with known concentration, with a final dye concentration of 4.98×10^{-5} M.

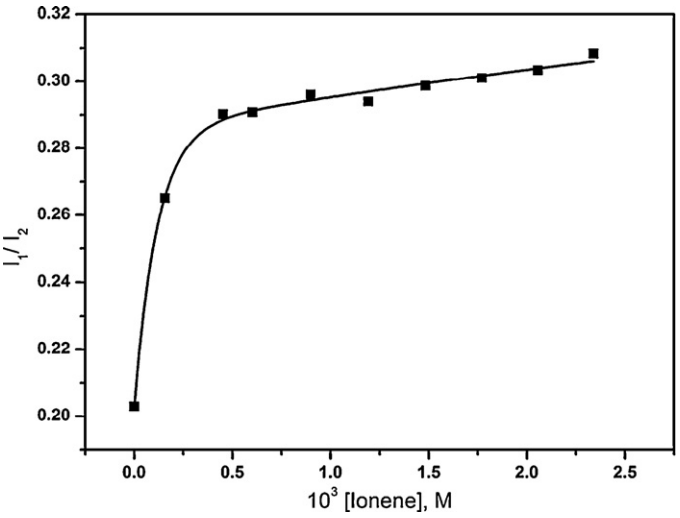

Fig. 1. Ratio of the absorbances of methyl orange at 372 nm (I1) and 464 nm (I2) as a function of the ionene [2-OH-33R4], 0.02 M borate and pH = 9.40 (for data see Table S.1).

3. Results and discussion

3.1. Characterization of the ionene nanoreactors

The absorption spectra of methyl orange has been proven to be a useful tool to investigate the nature of the hydrophobic environment in macromolecules because a non-polar environment significantly shifts λ_{max} to shorter wavelengths [30]. The absorption spectra of methyl orange changes as a function of concentration of the 2-OH-33R4 polyelectrolyte, with the absorbances increasing at 372 nm and decreasing at 464 nm as a function of the increase of [2-OH-33R4]. Fig. 1 shows that the intensity ratio of the absorption peaks has a large variation in ionene concentrations below 5×10^{-4} M, with a rather small change at higher concentrations. The small absorbance changes may be attributed to the partial incorporation of methyl orange in the ionene domain, with a significant shift to smaller wavelengths developing when the cationic polyelectrolytes are added to the solution. The observed effect of the 2-OH-33R4 on the spectra of the dye is suggestive of the induced formation of hydrophobic microdomains at low concentrations of polysoaps, and consistent with the assumption of Wang and Engberts [31], that the dye nucleates the formation of new aggregates.

When methyl orange is added to the more hydrophobic 2-OH-33R8, even for the lowest concentration of ionene, there is a significative shift of λ_{max} from 464 nm to 390 nm, indicating that the dye is totally incorporated in the ionene microdomains (Table 1).

3.2. Reduced viscosity

The concentration dependences of the reduced viscosity of the ionenes 2-OH-33R4 and 2-OH-33R8 in water are shown in Fig. 2. As expected for ionenes with R groups between methyl and butyl, the experimental behavior observed for 2-OH-33R4 is typical of polyelectrolytes, with the reduced viscosity increasing significantly as a function of the decrease in polymer concentration [32]. The observed effect is consistent with the fact that in solution, in the absence of salt, polyelectrolytes are in their elongated shape,

Table 1
λ_{max} of methyl orange as a function of 2-OH-33R8 concentration.

10^4 [monomer] (M)	λ_{max} (nm)
0.000	464
0.510	390
1.100	392
1.800	390
2.800	390
3.560	392
6.700	390
9.333	390
18.6	390
46.60	390

presenting high values of hydrodynamic volume. This is a consequence of the fact that with decreasing concentration of the ionene, the polymer expands because charges on the backbone are less shielded by counterions which increases repulsion. Probably, upon addition of salt, chains collapse into random coils due to charge screening of counter ions.

Conversely, as shown in Fig. 2, the more hydrophobic 2-OH-33R8 ionene behaves as a polysoap, with the reduced viscosity profile as a function of concentration being much less dependent on polymer concentration, consistent with a compact globular shape, corroborating results of dye incorporation.

3.3. Alkaline hydrolysis of PNPB in the presence of ionenes

The catalytic effect of functionalized ionene nanoreactors in the alkaline hydrolysis of PNPB was examined, initially, as a function of the concentration of hydroxide ion, data presented in Fig. 3, and the results show that the rate constant increases as a function of the concentration of added KOH showing a typical saturation-like profile with a reactivity order of 2-OH-33R8 > 2-OH-33R4 > 2-OH-33R1.

The experimental results shown in Fig. 3 for the alkaline hydrolysis of PNPB in the presence of the functionalized ionenes can be accounted by the reactions of (i) hydroxide ion in the aqueous phase ($[HO_w^-]$); (ii) hydroxide ion which concentrates in the ionene domain ($[HO_p^-]$) and (iii) alkoxide in the backbone of the ionene ($[RO_p^-]$), formed by ionisation of the 2-hydroxy substituent of the polysoap as a function of the increase in basicity in the ionene domain. The interactions between HO_w^-, HO_p^- and RO_p, are given in Scheme 1, where K_e is the deprotonation equilibrium of the ionene alkoxide by hydroxide ion (Scheme 1), and the pK_a values

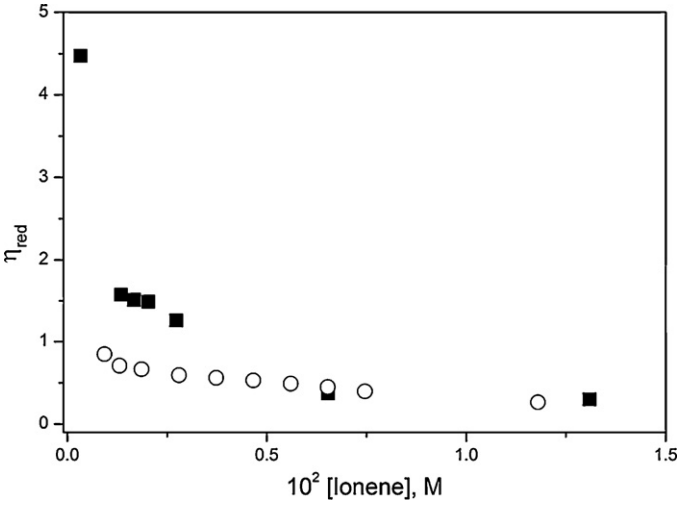

Fig. 2. Concentration dependence with the reduced viscosities for ionenes 2-OH-33R4 (■) and 2-OH-33R8 (○) in water (for data see Tables S.2 and S.3).

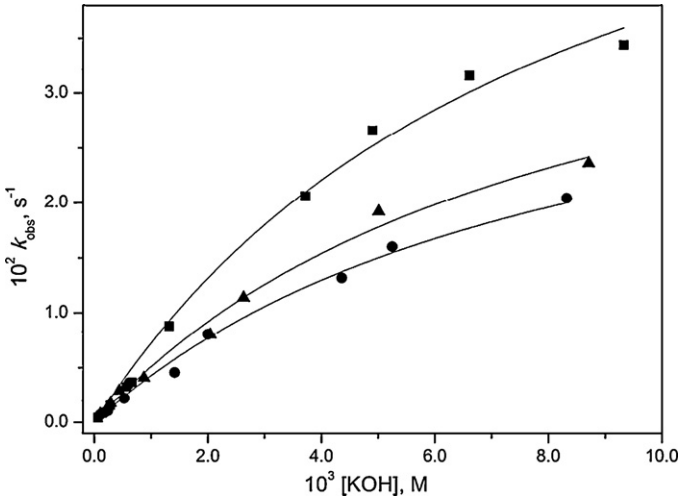

Fig. 3. Observed rate constants as a function of KOH concentration for the alkaline hydrolysis of PNPB, in the presence of 1.82×10^{-2} M 2-OH-33R1 (●); 1.48×10^{-2} M 2-OH-33R4 (▲) and 6.73×10^{-5} M 2-OH-33R8 (■). The points are experimental (for data see Tables S.7–S.9) and the solid line calculated according to Eq. (2).

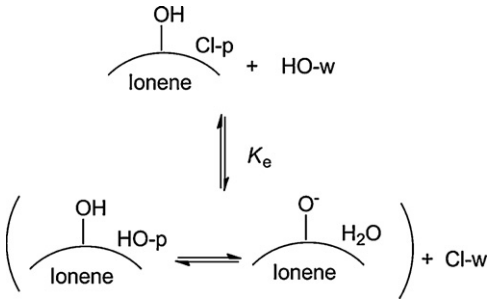

Scheme 1. Equilibrium reactions of the ionenes involving the hydroxide species in the aqueous phase ($[HO_w^-]$) and in the ionene domain ($[HO_p^-]$) and the alkoxide in the backbone of the ionene ($[RO_p^-]$).

for the ionenes can be estimated by means of Eq. (1).

$$K_a = K_w K_e \quad (1)$$

In order to obtain K_e from the kinetic profile shown in Fig. 3, the data were fitted with Eq. (2),

$$k_{obs} = \frac{k_{max} K_e [OH^-]_w}{1 + K_e [OH^-]_w} \quad (2)$$

where k_{max} corresponds to first order rate constant in the presence of the ionene nanoreactor and most probably contains contributions of both HO_p^- and RO_p^-. The solid lines in Fig. 3 represent the theoretical values calculated obtained by using Eqs. (1) and (2) and Table 2 summarizes the obtained rate and equilibrium constants. The value of k_{max} is slightly higher for 2-OH-33R8, and decrease with decreasing hydrophobicity of the ionenes. The pK_a values for the 2-OH-33R1 and 2-OH-33R4 ionenes are identical. The slightly smaller value obtained for 2-OH-33R8 is consistent with a more compact structure, where some electrical potential builds up and helps to concentrate hydroxide ion in the surface of the ionene.

Table 2
Calculated values of k_{max}, K_e and pK_a for the PNPB hydrolysis in the presence of 2-OH-33R1, 2-OH-33R4 and 2-OH-33R8.

Ionene	k_{max} (s^{-1})	K_e (M^{-1})	pK_a
2-OH-33R1	0.041	120	11.9
2-OH-33R4	0.046	123	11.9
2-OH-33R8	0.059	160	11.8

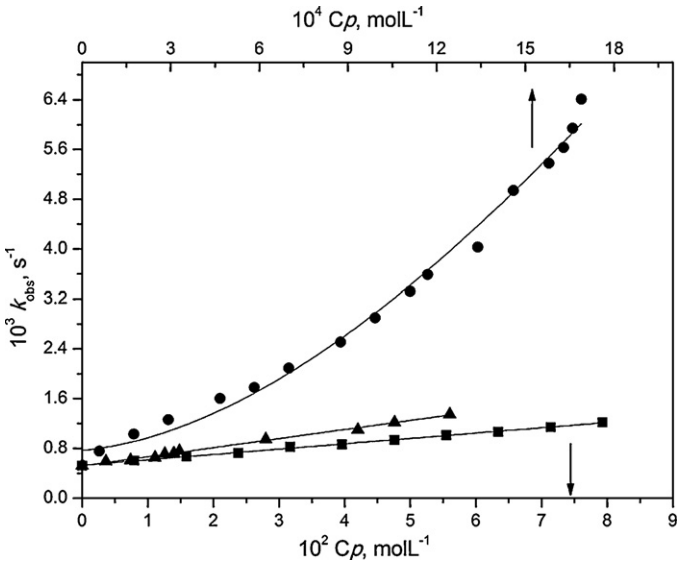

Fig. 4. Observed rate constants as a function of 2-OH-33R1 (■), 2-OH-33R4 (▲) and 2-OH-33R8 (●) concentration in alkaline hydrolysis of PNPB at pH = 10 (for data see Tables S.4–S.6). The points are experimental and the solid line calculated according to Eq. (3).

Besides, pK_a values in Table 2 show a behavior understandable when predicting pK_as for similar structures [33], and, for example, (dimethylamino) methanol has a pK_a of 14.87, for the acid dissociation of the OH group, hence the introduction of charged ammonium ions and hydrophobic groups (to a lesser extent) in neighboring positions results in a significant pK_a decrease. Although understanding this charge effect is not simple, the higher reactivity shown by the 2-OH-33R8 ionene may be due to both its lower pK_a and higher hydrophobicity.

The dependence of k_{obs} with the ionene nanoreactor concentration (C_p) was also evaluated and the rate constant profile is shown in Fig. 4 and, there is a linear dependence of the rate constant with C_p for 2-OH-33R1 and 2-OH-33R4. Conversely, the more hydrophobic 2-OH-33R8 shows a non-linear behavior probably related to more efficient binding of the substrate [34].

Moreover, compared to the reaction in the absence of ionenes ($k_0 = 5.25 \times 10^{-4}\ s^{-1}$, at pH 10), rate enhancements are 2- to 3-fold for 2-OH-33R1 and 2-OH-33R4 and 15-fold for 2-OH-33R8. These rate effects are significantly larger than those for the micellar mediated reaction of phenyl benzoate, where a small 1.5-fold rate increment was observed [35]. Besides, the effect is consistent with previous studies [28] which showed that, in the alkaline hydrolysis of benzoic anhydride, the rate constant in the presence of a non-functionalized ionene (poly[(dipropyliminium)-1,3-propanediyl bromide], 33R3) is accelerated with only 24% of the efficiency of the corresponding catalysis by the functionalized linear ionene nanoreactor (2-OH-33R1). All these reactions are fully consistent with Scheme 2, where alkaline hydrolysis of the substrate involves reaction of hydroxide ion in the aqueous phase

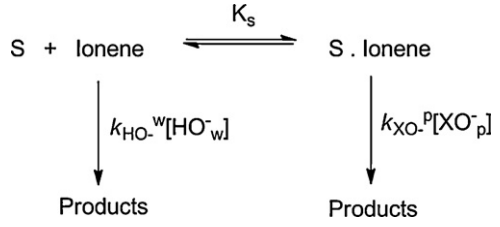

Scheme 2. Reactions in the aqueous and ionene nanoreactor domains.

Table 3
Calculated values of $k_{XO^-}{}^{p}[XO^-]K_S$ and $k_{HO^-}{}^{w}\left[HO^-\right]$ for the PNPB hydrolysis in the presence of 2-OH-33R1, 2-OH-33R4 and 2-OH-33R8.

Polymer	$10^3\ k_{XO^-}{}^{p}[XO^-]K_S\ (M^{-1}\ s^{-1})$	$10^4\ k_{HO^-}{}^{w}\left[HO^-\right]\ (s^{-1})$
2-OH-33R1[a]	8.60	5.30
2-OH-33R4[a]	14.60	5.19
2-OH-33R8[b]	7000	5.20

[a] Calculated using Eq. (4).
[b] Calculated using Eq. (3).

([HO_w^-]) or in the ionene domain ([HO_p^-]), or reaction with the alkoxide ion of the ionene ([RO_p^-]).

Clearly, the reactions of PNPB are mediated by the functionalized ionenes in this study and Eq. (3), which is consistent with Scheme 2, was used to fit the data in Fig. 4.

$$k_{obs} = \frac{k_{HO^-}{}^{w}\left[HO^-\right]_w + k_{XO^-}{}^{p}[XO^-]_p K_S C_p}{1 + K_S C_p} \quad (3)$$

In Eq. (3), $[HO^-]_w$ is the hydroxide concentration in water and $[XO^-]_p$ corresponds to the sum of the equilibrium concentrations of hydroxide ($[HO^-]_p$) and alkoxide ($[RO^-]_p$) ions in the ionene domain, defined as the molarity in the total solution. Therefore, the term $k_{XO^-}{}^{p}[XO_p^-]$ represents the contribution of both $k_{HO^-}{}^{p}[HO_p^-]$ and $k_{RO^-}{}^{p}[RO_p^-]$, which corresponds to the reactions of hydroxide ion and alkoxide ions in the ionene domain, respectively (Scheme 2). It is important to notice that at low ionene concentration, $1 > K_S C_p$, and Eq. (3) simplifies to the form shown in Eq. (4).

$$k_{obs} = k_{HO^-}{}^{w}\left[HO^-\right]_w + k_{XO^-}{}^{p}[XO^-]_p K_S C_p \quad (4)$$

It follows that a plot of k_{obs} versus C_p should be linear for low values of K_s and/or C_p. Indeed, this linear behavior was observed for the ionenes 2-OH-33R1 and 2-OH-33R4, and the data was fitted with this simplified equation and the calculated values for slope and intercepts are given in Table 3. With the more efficient 2-OH-33R8 ionene, a non-linear fit with Eq. (3) was necessary and calculated values of $k_{XO^-}{}^{p}[XO^-]K_S$ and $k_{HO^-}{}^{w}\left[HO^-\right]$ from fit of the data are also included in Table 3.

The calculated constant $k_{HO^-}{}^{w}\left[HO^-\right]$, included in Table 3, is consistent with previously reported rate constants for the alkaline hydrolysis of PNPB ($1.95 \times 10^{-4}\ s^{-1}$, pH 10, 33% acetonitrile in water) [36]. Since the calculated values of pK_a for the 2-OH-33R1, 2-OH-33R4 and 2-OH-33R8 are alike, within limits of experimental error, and the rate constants are only moderately affected by addition of organic solvents (see above), changes in K_s must be responsible for the observed dramatic increase in $k_{XO^-}{}^{p}[XO^-]K_S$. Thus, the results in Table 3 indicate that 2-OH-33R8 is a much better catalyst, by factors of about 815- and 480-fold than 2-OH-33R1 and 2-OH-33R4, respectively. Clearly, the higher hydrophobicity of 2-OH-33R8, facilitates the incorporation of PNPB more effectively in the ionene domains, promotes an increase in the association constant K_s and, therefore, a significant increase in catalytic ability.

All studied ionenes showed important catalytic effects, probably due to their ability to concentrate hydroxide ions ([HO_p^-]) a fact that is consistent with the similar pK_a values (Table 2) and to the fact that the alkoxide ion ([RO_p^-]) of the ionene is an effective nucleophile in the reaction. Recently, we reported the reaction of 2-OH-33R1 with benzoic anhydride, and showed that alkoxide attack occurs as shown in Scheme 3, which can be extended for reactions with PNPB. Deprotonation of the alkoxide (K_e, Scheme 1) is followed by two-step reactions (1) and (2), Scheme 3. In reactions with benzoic anhydride, the second step (2) is rate-determining, with breakdown of the acylated ionene intermediate taking about 6 h (in pH = 9). Similarly, in reactions of PNPB, the second step (2) is expected to be rate-determining, but this fact is not important

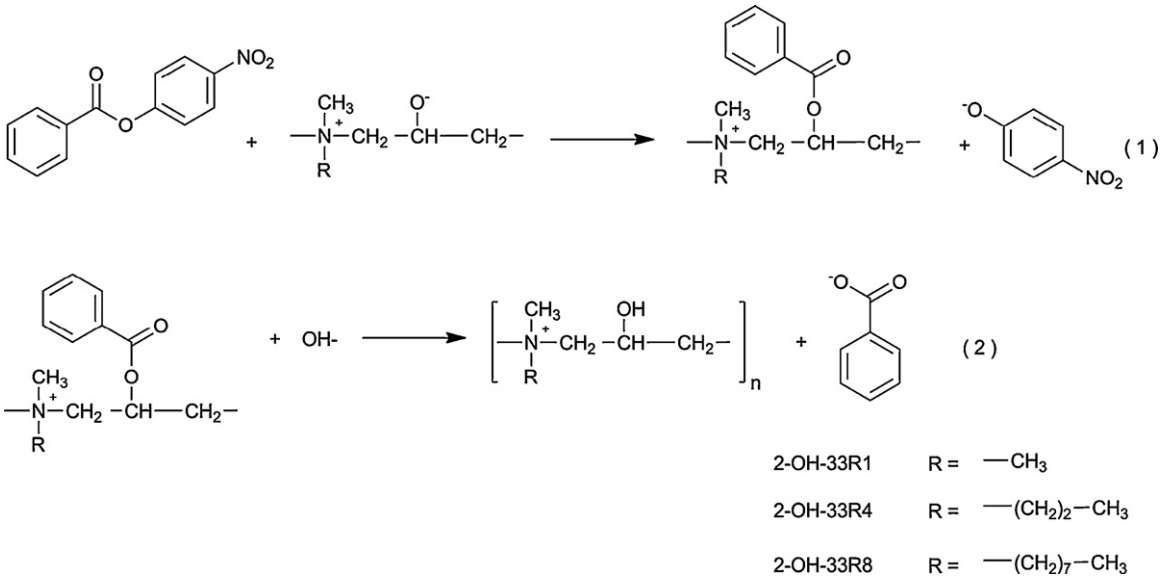

Scheme 3. Mechanism of PNPB hydrolysis in the presence of the ionene nanoreactors.

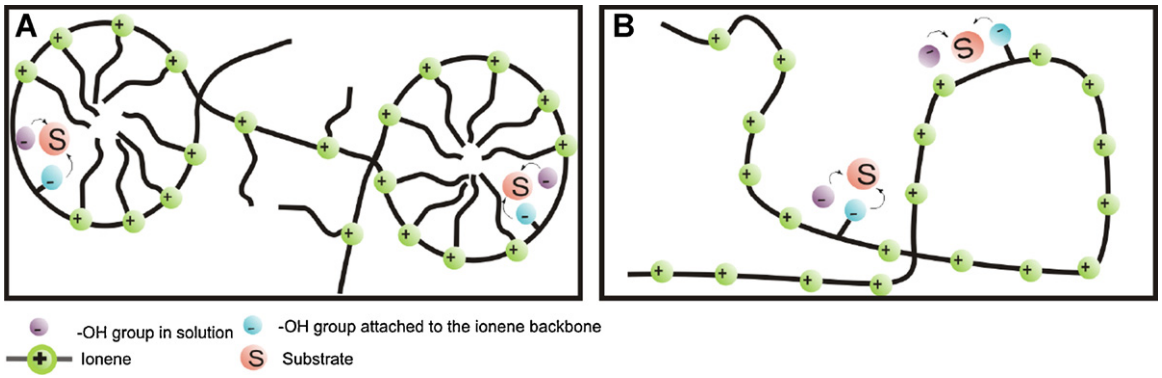

Fig. 5. Schematic of a small portion of a (A) polysoap molecule in aqueous solution where one can observe hydrophobic microdomains and free monomeric units, and (B) normal polyelectrolyte.

since the kinetic experiment were performed using a large excess of polymer and we only followed the p-nitrophenoxide liberation (reaction (1) in Scheme 3).

This result is not surprising since a p-nitrophenyl ester such as PNPB is expected to be hydrolyzed faster than the alkylbenzoate formed in the nanoreactor surface. These polysoaps are structurally closer to dendrimers than micelles and, in principle, could show turnover in reactions as do real catalysts in the presence of excess substrate provided the rate limiting step is the hydrolysis of the acylated nanoreactors 2-OH-33R1, 2-OH-33R4 and 2-OH-33R8.

The results suggest that alkaline hydrolysis of PNPB mediated by ionenes can occur as shown in Fig. 5, where (A) is the reaction in the presence of a polysoap which has the ability to form hydrophobic microdomains, thus acting as a microreactor concentrating reactants, and (B) is reaction in the presence of a normal polyelectrolyte.

4. Conclusion

Hydrolysis of PNPB in the presence of ionene nanoreactors was evaluated by comparing ionenes 2-OH-33R1, 2-OH-33R4 and 2-OH-33R8. Methyl orange incorporation and viscosity experiments showed that the increase of the ionene side chain promotes the ability of the polymer to form globular hydrophobic microdomains. This might explain the higher reactivity of 2-OH-33R8 toward PNPB hydrolysis compared to ionenes 2-OH-33R1 and 2-OH-33R4. Furthermore, 2-OH-33R8 has a slightly lower pK_a value and its lower pK_a may be a reflection of the higher hydrophobicity. The globular shape of the 2-OH-33R8 nanoreactor turns the catalysis particularly effective by increasing the ability of the ionene to concentrate HO^-_p and RO^-_p ions in the surface of the aggregates and, also binds the ester substrate in the interfacial region, behaving, as a consequence, like a catalytic homogeneous nanoreactor.

Acknowledgements

We thank INCT-Catálise and the Brazilian foundations CNPq, CAPES and FAPESC for financial assistance.

Appendix A. Supplementary data

Supplementary data associated with this article can be found, in the online version, at doi:10.1016/j.molcata.2010.09.002.

References

[1] A.J. Kirby, Acc. Chem. Res. 30 (1997) 290–296.
[2] F. Hollfelder, D. Herschlag, Biochemistry 34 (1995) 12255–12264.
[3] K.N. Dalby, A.J. Kirby, F. Hollfelder, Pure Appl. Chem. 66 (1994) 687–694.
[4] B.S. Souza, T.A.S. Brandao, E.S. Orth, A.C. Roma, R.L. Longo, C.A. Bunton, F. Nome, J. Org. Chem. 74 (2009) 1042–1053.

[5] A.J. Kirby, D.W. Tondo, M. Medeiros, B.S. Souza, J.P. Priebe, M.F. Lima, F. Nome, J. Am. Chem. Soc. 131 (2009) 2023–2028.
[6] W.B. Motherwell, M.J. Bingham, Y. Six, Tetrahedron 57 (2001) 4663–4686.
[7] L.J. Twyman, A.S.H. King, I.K. Martin, Chem. Soc. Rev. 31 (2002) 69–82.
[8] A.N. Zelikin, P. David, P. Shastri, R. Langer, V.A. Izumrudov, Bioconjugate Chem. 13 (2002) 548–553.
[9] F. Hollfelder, A.J. Kirby, D.S. Tawfik, J. Org. Chem. 66 (2001) 5866–5874.
[10] F. Hollfelder, A.J. Kirby, D.S. Tawfik, J. Am. Chem. Soc. 119 (1997) 9578–9579.
[11] M.S. Turner, J.F. Joanny, J. Phys. Chem. 97 (1993) 4825–4831.
[12] J. Villa, A. Warshel, J. Phys. Chem. B 105 (2001) 7887–7907.
[13] T. Rodulfo, J. Hamilton, E. Cordes, J. Org. Chem. 39 (1974) 2281–2284.
[14] L.R. Lawin, W.K. Fife, C.X. Tian, Langmuir 16 (2000) 3583–3587.
[15] L.S. Romsted, H. Cordes, J. Am. Chem. Soc. 90 (1969) 4404–4409.
[16] A.J. Sonnessa, W. Cullen, P. Ander, Macromolecules 13 (1980) 195–196.
[17] V. Soldi, N.M. Erismann, F.H. Quina, J. Am. Chem. Soc. 15 (1988) 5137–5143.
[18] W. Binana-Limbele, R. Zana, Macromolecules 23 (1990) 2731–2739.
[19] A. Dimov, E. Prodanov, S. Simeonov, Ekologiva 22 (1989) 30–34.
[20] E. Ranucci, P. Ferruti, N.M. Grazia, J. Bioact. Compat. Polym. 44 (1989) 403–409.
[21] E.C. Buruiana, T. Buruiana, J. Biomater. Sci. Polym. 15 (2004) 781–795.
[22] E.T. Kimura, P.R. Young, G.H. Barlow, Proc. Soc. Exp. Biol. Med. 111 (1962) 37–41.
[23] G.K. Noren, J. Polym. Sci. Polym. Chem. 20 (1975) 693–700.
[24] B. Gao, X. Zhang, Y. Sheng, Mater. Chem. Phys. 108 (2008) 375–381.
[25] D. Putnam, Nat. Mater. 5 (2006) 439–451.
[26] M.D. Brown, A.G. Schatzlein, I.F. Uchegbu, Int. J. Pharm. 229 (2001) 1–21.
[27] D. Luo, W.M. Saltzman, Nature 18 (2000) 33–37.
[28] A.C. Faria, R.S. Mello, E.S. Orth, F. Nome, J. Mol. Catal. A: Chem. 289 (2008) 106–111.
[29] V.L.A. Frescura, D.M.O. Marconi, D. Zanette, F. Nome, A. Blasko, C.A. Bunton, J. Phys. Chem. 99 (1995) 11494–11500.
[30] G.C. Hochberg, Colloid Polym. Sci. 272 (1994) 409–415.
[31] G.J. Wang, J.B.F.N. Engberts, J. Org. Chem. 59 (1994) 4076–4081.
[32] E.G. Knapick, J.A. Hirsch, P. Ander, Macromolecules 18 (1985) 1015–1021.
[33] Advanced Chemistry Development (ACD/Labs). Software V814 for Solaris (1994-2009 ACD Labs).
[34] T. Dwars, E. Paetzold, G. Oehme, Angew. Chem. Int. Ed. 44 (2005) 7174–7199.
[35] R. Germani, G. Savelli, N. Spreti, G. Cerichelli, G. Mancini, C.A. Bunton, Langmuir 9 (1993) 61–65.
[36] J.F. Kirsch, W. Clewell, A. Simon, J. Org. Chem. 33 (1968) 127.